

Light Metals 2015

**ALUMINUM ALLOYS:
DEVELOPMENT,
CHARACTERIZATION
AND APPLICATIONS**

Deformation and Texture

SESSION CHAIR

Xiyu Wen

University of Kentucky
Lexington, KY, USA

Evaluation of Forming Limit Diagram of Aluminum Alloy 6061-T6 at Ambient Temperature

Manoj K Sharma¹, J Mukhopadhyay²

^{1,2} Materials Science & Engineering Department Indian Institute of Technology Gandhinagar, Ahmedabad, Gujarat, 382424, India

Keywords: FLD, DIC, Speckle pattern, Hills-Swift model

Abstract

As fuel price increases, automobile industries are looking for more fuel efficient cars with less carbon emissions and high crashworthiness. Accordingly, this has necessitated for further research into the formability of Al 6xxx series alloys that have low weight and high strength properties. Since Al 6xxx series alloys are used in automotive panels, their formability characterization is essential. Hence, it is important to study the Forming Limit Diagram (FLD) which predicts the limit strains which in turn, can be imposed safely during forming. The present work mainly focuses on determining the Forming Limit Diagrams of Al6061-T6 alloy experimentally. The measurement of limit strains was accomplished using Digital Image Correlation Technique. The Hill - Swift model was used to predict FLD theoretically and a good agreement was found with the experimental results. Experimental results show that the use of appropriate formability parameters and reasonable processing methods can improve formability of Al6061-T6 alloys.

Introduction

During world war II, steel and cast iron were used for engineering applications because they have good strength and hardness along with other attractive properties, but transportation by road, air and ship has become more important in day to day life. Therefore, we need to develop alloys of low density, which have good strength to weight ratio. Aluminum, because of its low density is considered as one of the light weight metals. Presently, the automobile industry, mainly focuses on light weight and fuel efficient vehicles. Their main challenge is to reduce energy consumption and air pollution. A 10% weight reduction in automobile vehicle saves approximately equivalent to 5.5 % improvement in the fuel efficiency [1].

Aluminum is comparatively the best to make light weight with regard to strong vehicles among all different light metals available so far. Aluminum alloys have excellent strength-to-weight ratio, corrosion resistance, recyclability, ductility and durability, formability etc. A unique combination of these properties makes aluminum the best metal among all others to use in automotive and aerospace industries. Previously, several automotive industries used steel as dominant material. Aluminum has density only one-third that of steel which makes aluminum replace steel in automobile sector [2]. Presently, most of the industries work on zero waste. Aluminum has good recyclability and during recycling, around 95% of energy can be saved which also reduces the air pollution.

The forming limit diagram is a plot between the major and minor strains. The first diagram was published by Keeler in 1961 [3]. This diagram determines only the positive range of the minor strain. Subsequently, in 1968, new forming limit diagram was determined by Goodwin, Hence, forming limit diagram is also called as Keeler-Goodwin diagram [4]

Differences of Aluminum and Steel Sheets

The normal anisotropy value (r - value) of steel is larger than unity, whereas aluminum has an (r - value) smaller than unity. This affects the final shape and thus causes variations in the steel and aluminum sheets upon forming. Therefore, the thickness variations of these materials for the same drawing operations may be different. Excessive thinning or thickening problems may arise which may even lead to failure of these materials during uncontrolled manufacturing processes.

Aluminum is having one-third elastic (Young's) modulus as compared to steel, making the spring back effects more dominant. Therefore, elastic recovery poses a greater problem for aluminum sheets. The residual stress distributions become completely different compared to steel, affecting partial response to successive operations and product life. Furthermore, aluminum and steel materials have different strain hardening coefficients, leading to different strain hardening behaviors. The final surface qualities of aluminum and steel sheets are different due to different grain structures giving rise to different surface properties.

Experimental Method for Obtaining the FLD

Experimental method involved stretching of different specimens of different width. By varying the width of the specimen, the lateral constraint (i.e. the amount of material allowed to draw into the die cavity in the width direction) could be carried out to achieve failure in modes ranging from uniaxial tension through plane strain of balanced biaxial tension. Sheet metal forming machine has been shown in figure 1 that was available at forming lab of IIT Bombay. Blanks were cut in the desired direction in length of 200 mm for each of the following test widths: 25 mm, 50 mm, 75 mm, 100 mm, 125 mm, 150 mm, 175 mm and 200 mm.



Figure 1. Hydraulic press (Courtesy: IIT Bombay)
A circular grid pattern of 2.5 mm was made on the surface of the sample while using an Electrochemical etching method, Screen

printing method, Photochemical etching method and Laser etching method. In the present work, a digital image correlation (DIC) technique was used. DIC was necessary, as it provided ease in gaining useful information about materials that involved processes that occur at the micro level. As a result, testing methods were required to have a desired resolution and thus, capture the results after the sample was cut. In DIC technique, a speckle pattern was required, which has been shown in figure 2. Speckle pattern is required in order to distinguish between various types of sample available, otherwise it becomes difficult to find a deformation point on the sample given. Speckle patterns are usually made up of black and white paints. With the help of DIC, it was easier to calculate velocity, displacement, acceleration, stress and strain. DIC was a 3-D, non-contact optical technique to measure deformation and strain on the aluminum samples. This technique can be used for various tests. In DIC, very high speed cameras with resolution up to 1,000,000 frames/sec were used.

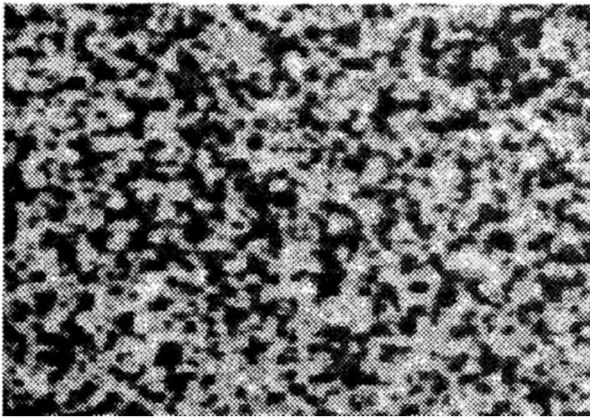


Figure 2. Speckle pattern

DIC Results with Different Sample Sizes

The right hand side of the FLC is obtained by subjecting the blank to biaxial stretching. This is achieved by holding the specimen, while being formed, around the entire boundary by the lock-bead. Such a specimen will henceforth be referred to as a full width specimen. The left hand side of the FLC is obtained by reducing the widths of the specimens. NADDRG recommends a rectangular shaped blank for reduced width specimens [64].



Figure 3. Fracture of reduced-width rectangular specimen during the test

However, rectangular specimens of the aluminum alloys tested here are found to fail at the bend radius of the lock bead due to stress concentration and when blank holder force is large, then the metal will not flow properly into the die cavity, hence it causes lock bead failure. As seen in figure 3, several experiments with different design conditions are performed. Figure 4 shows specimens of different widths used in the tests.



Figure 4. Deformed sample (a) sample of 200x200 mm² deformed SM; (b) A sample of 200x100 mm² deformed SM

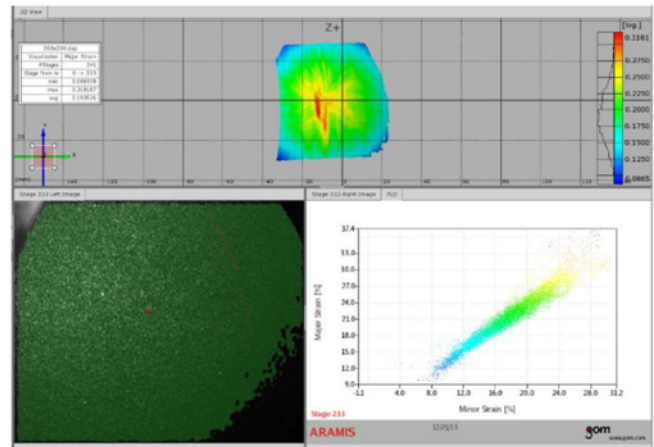


Figure 5. DIC Results 200x200 mm² samples

Figure 5 shows the biaxial stretching of sample 200 x 200 mm². Red color indicates the crack in the sheet, green show the safe side, i.e., no signs of crack formation and yellow indicates the formation of cracks. Failure in this sample starts at the center point of the sheet. This result is calculated by DIC. Limiting strains are determined for 1.5 mm thick Aluminum 6061-T6 sheets under a range of forming conditions (strain states and punch speed). For each combination of forming speed and blank width, different strain paths are obtained by forming samples of different widths.

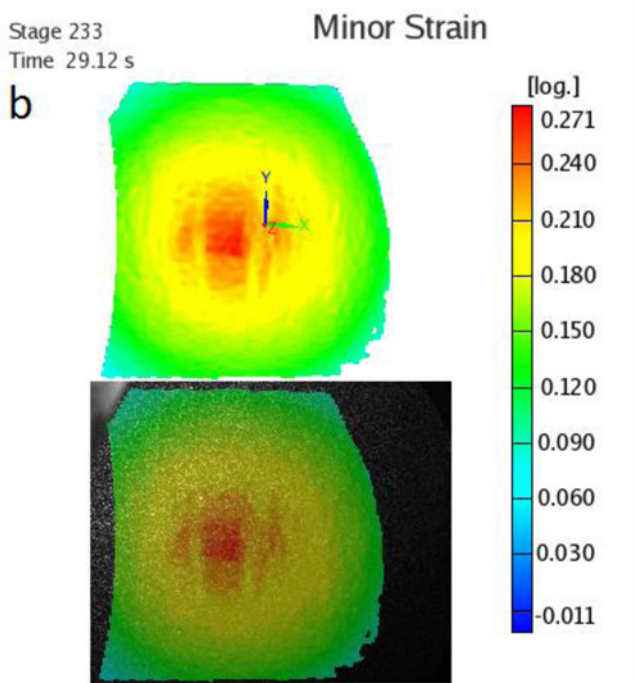
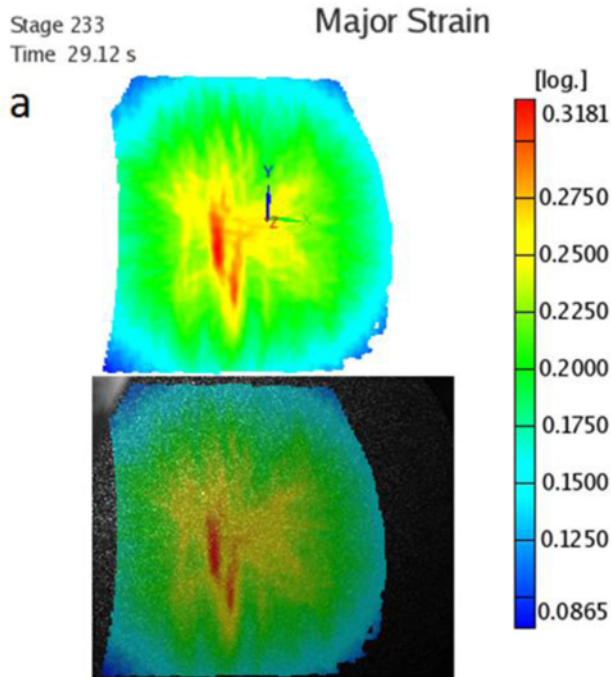


Figure 6. 4.13: DIC results 200x200 mm² samples (a) major Strain and (b) minor strain

Figure 6 shows that major strain is always greater than the minor strain even when tensile force is applied in both the cases. Figure 6 (a) & (b) indicates equal biaxial stretching, which shows that sheet stretched over a hemispherical punch deforms the sample at its center.

Effect of Sample Geometry

Material blank is cut in the desired direction in length of 200 mm for each of the following test widths: 25 mm, 50 mm, 75 mm, 100

mm, 125 mm, 150 mm, 175 mm, 200 mm. In order to construct FLDs, values are measured in response to a range of forming parameters. Results corresponding to forming speeds of 5 mm/min are presented here at different width samples. Dome height increased with the decrease in sample width. This increase is attributed to enhance the material flow in the transverse direction and diffuse necking, which is greater for smaller sample widths. Negative effects are more significant for sample of larger widths. It is reported that sheet orientation has very little effect on formability in the plane strain state, but can have large effects on uniaxial tension or in the drawing region, i.e. the negative minor strain region. The tests are performed by using samples cut in the rolling direction (RD) and transverse direction (TD). Specimens with minimum widths of 25 mm, 50 mm and 75 mm (oriented in both the RD and TD) are used with Teflon sheet lubricant and stretched at a punch speed of 5 mm/s and clamping force of 25 kN. FLDs are measured by inspecting for necking with the images captured by the DIC system and the results are shown in Figures 7 (a), 7 (b), 7 (c), 7 (d), 7 (e), 7 (f), 7 (g), and 7 (h). In general, rolling-oriented samples are higher for limiting dome heights for strain states in the negative minor strain region. This effect can be attributed to the aspect ratio of grain size of the material. This agrees with the fact that a larger difference between R-values is found at room temperature for RD samples than TD samples.

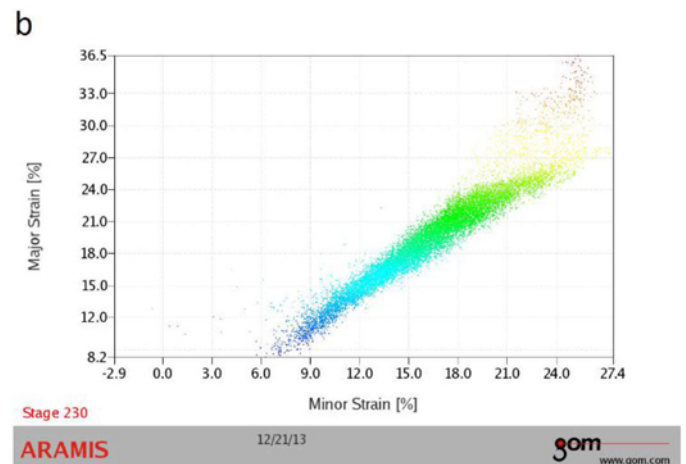
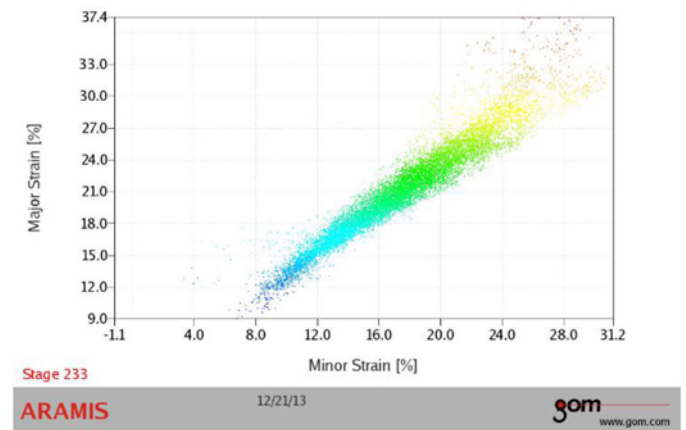


Figure 7. Major strain with minor strain for samples, with (a) 200 mm (b) 175 mm (c) 150 mm (d) 125 mm (e) 100 mm (f) 75 mm (g) 50 mm and (h) 25 mm with constant length (continued)

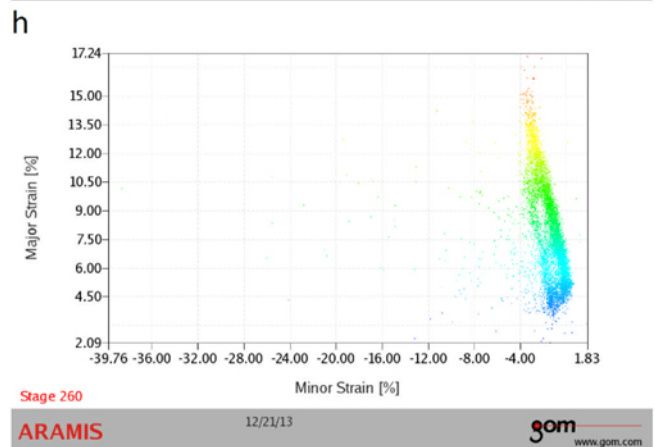
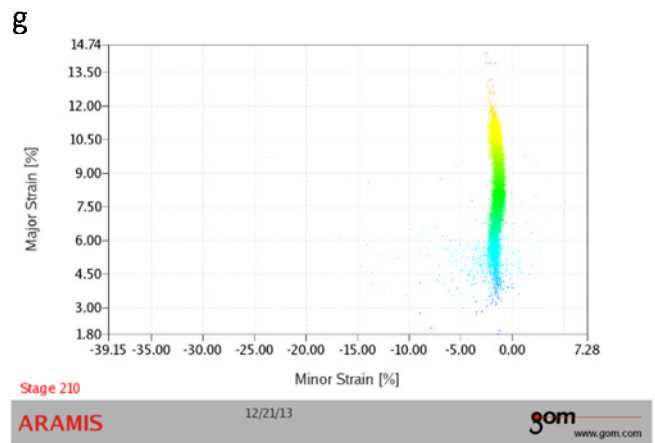
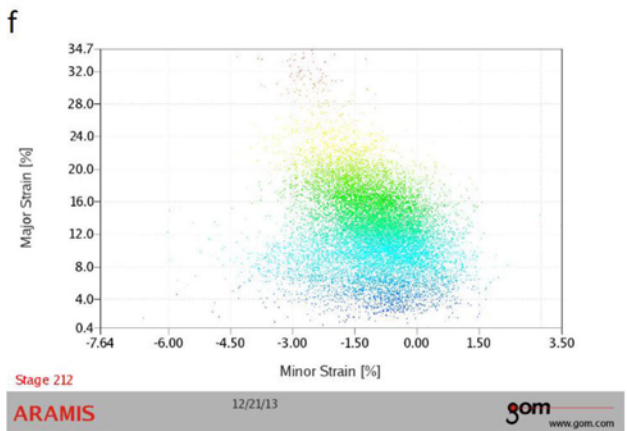
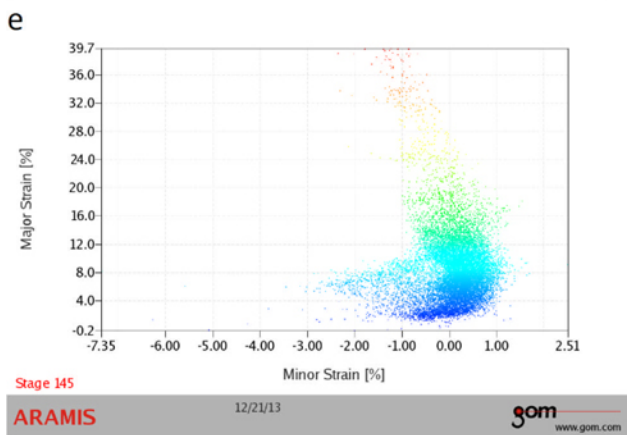
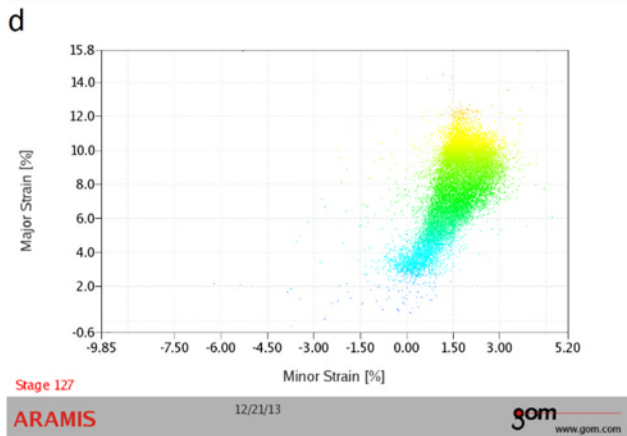
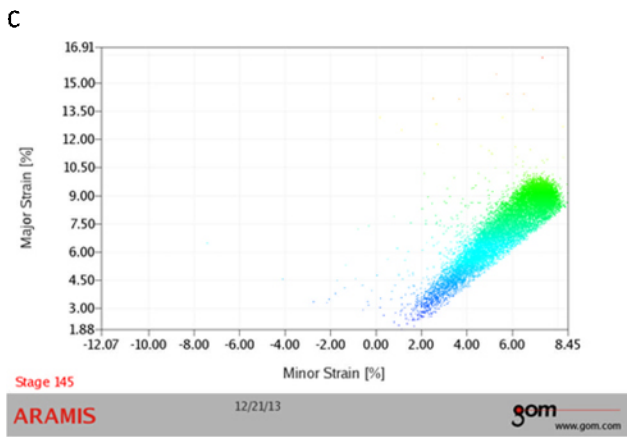


Figure 7. Major strain with minor strain for samples, with (a) 200 mm (b) 175 mm (c) 150 mm (d) 125 mm (e) 100 mm (f) 75 mm (g) 50 mm and (h) 25 mm with constant length.

The element of necking is thus identified and the corresponding element in the Optical Measuring Techniques contour plot is also observed. Therefore, an FLD is plotted for 5 mm/min as shown in Figure 8. It shows that the FLC for 1.5 mm thick Aluminum 6061-T6 sheet along with the strain data points from each of the different specimens that are used to generate it. It is noted that with the in-situ observation technique, the strains are calculated while the specimen is still loaded (i.e., the punch is still in contact with the specimen such that the elastic strains in the sheet are not released). The average number of images captured for typical test is about 180 images (90 from each of the 2 cameras). This huge number of frames are needed in order to be able to detect the onset of localized necking. An image just before when the necking happens is selected as the last image to be analyzed. A facet size of 31 pixels and step size of 29 pixels is used to perform the DIC. A facet size of 31 pixels corresponds almost to 2.5mm on the surface of the blank, which is close to the size of the circular grid used in the conventional strain circle technique. A step size of 29 pixels indicates that the distance between the centers of adjacent facets is 29 pixels. The overlapping of adjacent facets helps in pattern matching for the two images obtained from different angles. The "step" method (i.e., the total deformation is obtained by comparing successive images on a step-by-step basis) is used for the analyses such that strains are obtained in all stages of the forming process. The "multi-facet" option is used to analyze the images since it yields a higher accuracy.

Major and minor strain values for each facet for the final stage of deformation are exported and plotted using MS-Excel to generate the FLD of a particular test, as shown in Figure 8. This is taken to be the limiting strain. A set of such limiting strain points found in a similar manner from full width specimens with different friction conditions and reduced width specimens of various widths defines the FLC for a given material. Forming limit curves are determined by using the procedure described above for 1.5 mm thick Aluminium-T6 sheets. It shows that the FLC for 1.5 mm thick Aluminium-T6 sheet along with the strain data points from each of the different specimens that are used to generate it. It should be noted that with the in-situ observation technique, the strains are calculated while the specimen is still loaded (i.e., the punch is still in contact with the specimen such that the elastic strains in the sheet are not released). In the traditional method the specimen is removed from the tool and allowed to spring-back before measuring strains. The strain measured for a loaded blank will be higher than the strain measured after releasing the load. The fact that the test is not aborted, results in FLCs that are less traditional (more realistic) than those obtained using the conventional method.

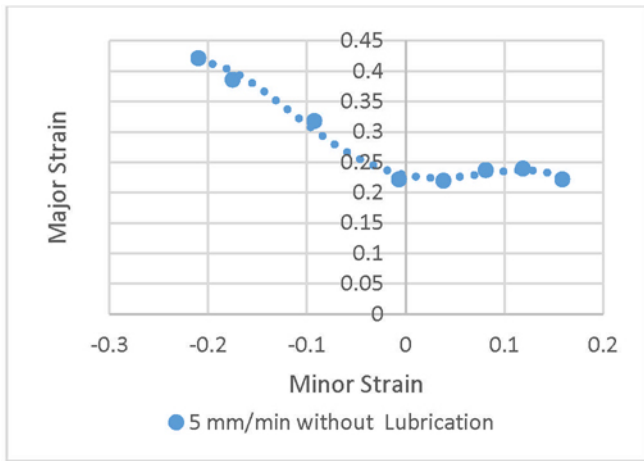


Figure 8. Forming Limit Diagram, 5 mm/min punch speed without using any lubricant

Prediction of failure during drawing is possible by constructing forming limit diagrams. Major and minor strains found from the DIC can also be predicted if the sheet has undergone thinning or not. After a number of such tests, the forming limit diagram is drawn, between major strain and minor strain. The boundary between safe and break down regions are represented in the forming limit diagram. Any strain represented in the diagram by a point lying above the curve indicates the failure. The strain path can be varied depending on the width of the sheet. The higher the position of the curve greater is the formability. In this diagram, a few straight lines indicate strain paths. The vertical line at the center (zero minor strain) represents a plane strain. In biaxial strain, both strains are equal. This is represented by the inclined line on the right side of the diagram. Simple uniaxial tension is expressed on the left side by a line with slope 2:1. This is due to the case that Poisson's ratio for plastic deformation is half. Negative minor strain means there is a shrinkage. It is desirable to have a negative minor strain because the major strain to failure is higher for the negative values of minor strain. Some of the factors which affect the forming limit of a material are strain rate sensitivity, anisotropy, thickness of the sheet, strain hardening etc. The forming limit curve shifts upwards as the sheet thickness increases.

Identification between the Experimental and Theoretical FLD

The values of n , R_0 , R_{45} , R_{90} and average anisotropy factor (r), which are used in the theoretical determination of FLD, and their values are determined by tensile test are shown in table (1).

Table 4.1: Property of sheet metal of Aluminum 6061-T6

Angle to rolling direction Aluminum 6061-T6			
Parameters	0°	45°	90°
Ultimate tensile stress (MPa)	266	287	281
Module of elasticity (MPa)	31396.96	23583.31	24182.16
Maximum force (Newton)	2401.89	2586.45	2582.63
Total elongation (%)	19	18	19
Anisotropy factor (r)	0.48	0.7	0.53
Strain-hardening exponent (n)	0.17	0.18	0.16
Average strain-hardening exponent (n)	0.17		
Average Anisotropy factor (r)	0.60		

Figure 9 and 10 represent the effect of grain orientation on the formability of Aluminum 6061-T6 sheets. It is observed that grain orientation has very little effect in the zero minor strain region while it is influential in the negative minor strain region of the n and r with the 45° orientation specimens having the highest value of limiting strain. Similar results are observed from the tensile test, where the limiting strain is nearly the same in the plane strain region for all grain orientations, whereas in the negative minor strain region the effect of sheet orientation is evident. The 45° orientation has the highest limiting strain for the points in the negative minor strain region.

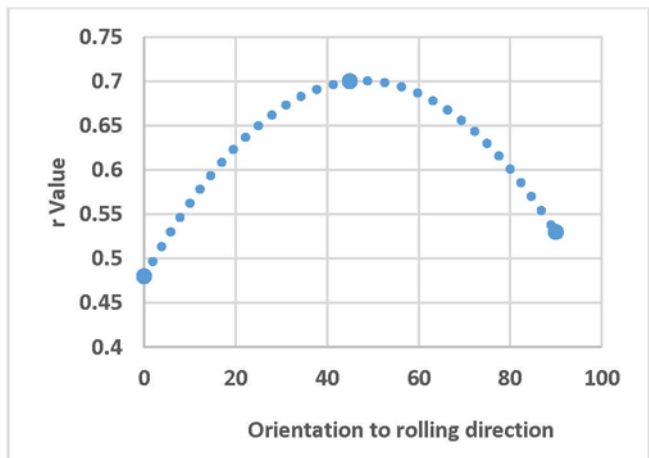


Figure 9. Variation of r-value vs. rolling direction for a 1.5 mm Aluminum 6061-T6

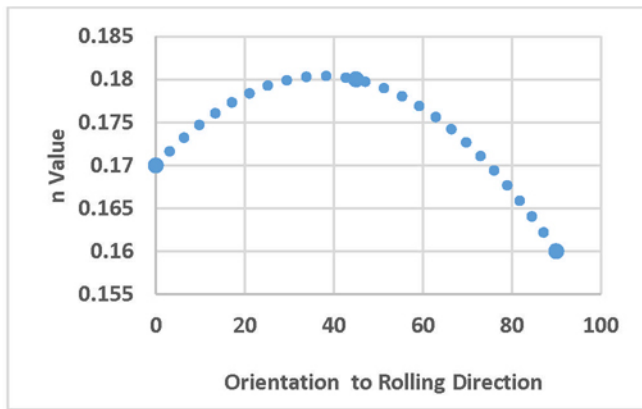


Figure 10. Variation of n-value vs. rolling direction for a 1.5 mm Aluminum 6061-T6

Figure 11 shows the theoretical forming limit diagrams using Hill-Swifts model. It can be seen that this analysis overestimates the limit strain towards the equi-biaxial strain path and underestimates the limit strains towards the plane strain and uniaxial regions. One of the most important factors for prediction of FLD through the Hill-Swifts model is the applied constitutive model. Figure 11 presents the experimental and numerical forming limits for Aluminum 6061-T6 alloy and thus provides an experimental and theoretical analysis for the determination of the FLD using Hills - Swifts model for the Aluminum 6061-T6 alloy. The experimental results are compared with the Hills-Swift model and results are found to be in a good agreement.

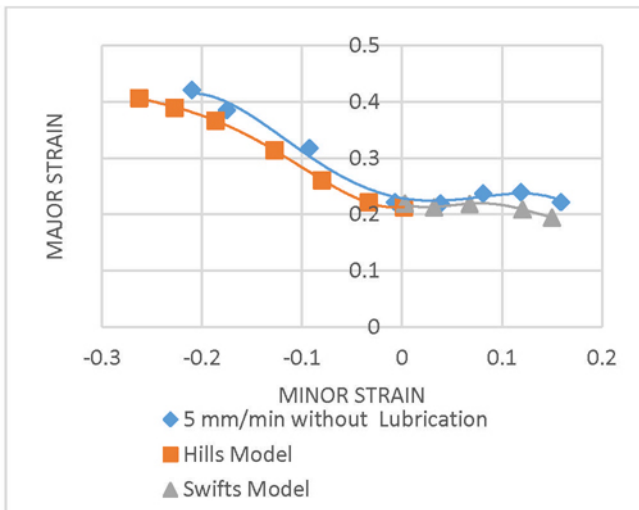


Figure 11. Experiment versus model for FLD

Conclusion

- I. Formability is critical consideration for selecting the suitable recycle friendly aluminum alloy for automotive applications.
- II. Aluminum 6061-T6 is found to be suitable for automotive components and this alloy can be used as light weight substitute for steel which is currently used.
- III. It is observed that with the increase of die corner radius, the limit strain increases. The blank holding force has no impact on the values of limit strain and forming limit diagram.

- IV. Even though the safer deformation zone decreases with the increase of blank holding force, the limit strain is independent of blank holding force when the ratio of principal strain is low.
- V. Lubrication increases formability in both the left and right-hand-sides of the FLC. Teflon lubricant is more effective at room temperature.
- VI. The FLD test and in-situ 3D DIC are used to determine the FLCs for 1.5mm thick aluminum sheet. With in-situ strain measurements, the limit strains can be determined with a better accuracy. Furthermore, the evolution of strain can also be tracked throughout the forming process.
- VII. The values limit strain are found to increase with the increase of sheet thickness
- VIII. Finally, FLD obtained experimentally is compared with FLD obtained theoretically using the Hills-Swift model and the results are found to be in a good agreement.

References

1. A. Morita, Aluminium alloys for automobile applications, in: Proc. of. ICAA-6, Toyohashi, Japan, 5–10 July 1998, in: Aluminium Alloys, vol. 1, 1998, pp. 25–32
2. Gesing, Adam, et al, "Separation of Wrought Fraction of Aluminum Recovered from Automobile Shredder Scrap," Light Metals 2001, TMS, Warrendale, PA, 2001.
3. Gesing, Adam, Larry Berry, Ron Dalton, Richard Wolanski, Huron Valley Steel Corporation, "Assuring Continued Recyclability of Automotive Aluminum Alloys," Light Metals 2002, TMS, Warrendale, PA, 2002.
4. Goodwin, G.: Application of strain analysis to sheet metal forming problems in the press shop, Society of Automotive Engineers, No. 680093. (1968) pp. 380-387
5. Woodthorpe J, Pearce R (1970) The effect of the r and n upon the FLD of sheet steel. Proceedings of the ICSTIS Conference, Tokyo, 822–827
6. Narashimhan K, Nandedkar VM (1996) Formability testing of sheet metals. Transactions of the Indian Institute of Metals 49:659–67
7. S. Holmberg, B. Enguist, P. Thilderkvist. Evaluation of Sheet Metal Formability by Tensile Tests. Journal of Material Processing and Technology, 145:72-83, 2004.
8. Miles M (2006) Formability testing of sheet metals. In: Semiatin SL (ed) ASM handbook, Vol 14B, Metalworking: Sheet metal. ASM International, Materials Park, OH, 673–698
9. H. Noori and R. Mahmudi, Prediction of Forming Limit Diagrams in Sheet Metals Using Different Yield Criteria, Metall. Mater. Trans. 38A (2007) 2040-52.